Closed-form solutions to optimal parameters of dynamic vibration absorbers with negative stiffness under harmonic and transient excitation

Shaoyi Zhou, Claire Jean-Mistral, Simon Chesné

Version of Record: https://www.sciencedirect.com/science/article/pii/S0020740319302127
Manuscript_f6d762fea551a692cfdfbb0cbf2d3a44

Closed-form solutions to optimal parameters of dynamic vibration absorbers with negative stiffness under harmonic and transient excitation

Shaoyi Zhou, Claire Jean-Mistral, Simon Chesne*

Université de Lyon, CNRS INSA-Lyon, LaMCoS UMR5259, 69621 Villeurbanne, France

Abstract

In this present paper, two configurations of dynamic vibration absorber in conjunction with negative stiffness (NSDVA) are investigated and their parameter optimization is conducted according to two tuning methodologies: the fixed points theory and the stability maximization criterion. Closed-form solutions to the optimal parameters of NSDVAs are analytically derived and are expressed in terms of ratio between the negative stiffness and mechanical stiffness of primary system. Allowable bounds on negative stiffness are specified with the consideration of stability requirement, based on which the ultimate control performance of NSDVAs could be imagined. Furthermore, an optimal negative stiffness ratio is defined within the stable region when the NSDVAs are tuned by the fixed points theory. Finally, numerical simulations are carried out in both harmonic and free vibration scenarios. Simulation results suggest that the inclusion of negative stiffness in the coupled system can significantly improve the vibration control performance in terms of broadening the frequency bandwidth of vibration suppression, decreasing the peak vibration amplitude of primary system and confining the stroke length of NSDVAs. Meanwhile, the negative stiffness can enhance the damping capability of coupled system, engendering an accelerated convergence of transient disturbances.

Keywords: Dynamic vibration absorber, negative stiffness, optimization, fixed points theory, stability maximization criterion

1. Introduction

In the fields of mechanical and civil engineering, the dynamic vibration absorber (DVA) is widely used to reduce the undesired detrimental effects of dynamic loads on primary systems for its high simplicity and reliability [1–4]. Conventional DVAs are purely passive and are composed of three common mechanical elements, i.e. mass, spring and viscous damper. The traditional DVA (denoted as DVA-I in this paper) was proposed and well documented in [5], whose mass is attached to the primary structure via a parallel connection of a linear spring and damper. Meanwhile, a non-traditional DVA (denoted as DVA-II) was developed in [6], whose damper is connected to the base instead of the main system.

The first analytical method for tuning DVAs is the fixed points theory [5]. In the objective of minimizing the peak amplitude of frequency response function (FRF) of primary system, it consists in equalizing the vibration amplitude at fixed points and making the FRF passing horizontally through these points. In fact, the fixed points correspond to positions where all FRFs of undamped primary system intersect, regardless of the damping level of DVA. Clearly, this heuristic approach only yields an approximate solution to the H_∞

*Corresponding author
Email address: simon.chesne@insa-lyon.fr (Simon Chesne)

optimization problem due to the discrepancy between fixed points and resonance peaks of FRF, however, its high accuracy and efficiency is a long established fact [7]. By applying the fixed points theory, the optimal tuning of DVA-I and DVA-II was accomplished by Den Hartog [5] and Ren [6], respectively, when connecting to an undamped primary system of single degree of freedom (SDOF). It was reported in [6] that compared to DVA-I, DVA-II can slightly improve the vibration control performance and could bring convenience in certain practical implementation. For damped primary systems, approximate solutions were carried out for optimal parameters of DVA-I [8] and DVA-II [9] by employing an equivalent linearisation technique, by means of which the damped primary system can be matched with an equivalent undamped one.

When the main system undergoes a transient disturbance, however, the optimal tuning based on fixed points theory could loss its effectiveness, since it aims at improving the steady state frequency response. In this context, a new tuning rule, termed as stability maximization criterion, was proposed by Yamaguchi [10] in the objective of decaying the transient disturbance as soon as possible. The design objective is fulfilled by maximizing the minimal absolute value of the real parts of system eigenvalues. By using this method, Yamaguchi [10] determined the optimal parameters for a DVA-I attached to an undamped primary structure. Xiang and Nishitani [11] analytically formulated the optimal parameters of DVA-II for an undamped main system, meanwhile, provided numerical solutions for a main system with different damping values.

Nevertheless, the disadvantages of DVA-I and DVA-II are evident. First, their vibration control performance is limited by the maximally attainable mass ratio between the DVA and main system. Second, both DVAs are only effective within a narrow frequency range around the target mode, whose control effect could deteriorate when the excitation frequency varies. In the objective of enabling DVAs to adaptively track the excitation frequency, smart materials whose physical properties are adjustable can be integrated, e.g. shape memory alloy [12, 13], magnetorheological elastomer [14, 15] and combination thereof [16]. Besides, it was reported in [17] that the negative stiffness can be used to enhance the vibration control performance.

The negative stiffness mechanism (NSM) is featured by a force-displacement curve with a negative slope, signifying that a NSM can generate a force to assist its motion instead of resisting it. Recently, the NSM has received wide attention in the domain of vibration isolation. By arranging in parallel the NSM and the support stiffness of structure to be isolated, the resonance frequency can be decreased, thereby improving the vibration isolation in the low-frequency region and broadening the frequency range of vibration isolation, meanwhile, the static stiffness is not affected in avoidance of an excessive static deflection and system instability. The high-static-low-dynamic stiffness characteristics can be achieved by various mechanical structures, which can be categorized into: symmetric pre-compressed springs [18, 19], bio-inspired X-shaped structures [20, 21] and magnetic negative stiffness springs [22, 23]. Clearly, most NSMs in aforementioned researches are passive and nonlinear, meanwhile, it was stated in [23] that the negative stiffness utilizing Maxwell magnetic normal stress can be regarded as linear in a certain range around the equilibrium position. A more convenient approach to realize a linear NSM was proposed and experimentally validated in [24] by using an active control technique with a linear actuator. To summarize, the NSM has widespread application in ameliorating the vibration isolation performance, however, only few studies on enhancing the control effect of DVAs via negative stiffness are available in the literature, as reported below.

Shen et al. [25] incorporated a negative stiffness between the base and the mass of DVA-II, yielding the NSDVA-II configuration. Its optimization according to the fixed points theory was carried out for a SDOF primary system, suggesting that the use of negative stiffness decreases the peak vibration amplitude of primary

system and broadens the frequency range of vibration absorption. Similarly, the NSDVA-I was studied by Antoniadis et al. [26], however, the optimal damping value of absorber had not been provided. Later, Huang et al. [27] also addressed the optimal tuning of NSDVA-I attached to a SDOF primary system, while the optimal damping value of absorber was derived according to the equal damping criterion proposed in [28]. This criterion yielded a larger damping value for DVA and a larger peak amplitude for primary system when compared to the case optimized by the fixed points theory. It should be mentioned that the intentional introduction of a grounded negative stiffness into both DVAs does contribute to the improvement of vibration control performance, meanwhile, the coupled system could be potentially destabilized. Nevertheless, the crucial stability analysis and the permissible interval of negative stiffness had not been addressed in aforesaid works and the NSDVAs had been optimized only in terms of suppressing harmonic vibration.

Therefore, the focus of this present paper is to carry out a thorough optimization analysis for both types of DVAs enhanced by grounded negative stiffness, NSDVA-I and NSDVA-II, under harmonic and transient excitation circumstances. Coupled systems related to both NSDVA-I and NSDVA-II are nondimensionalized in the same framework. Then, their optimal parameters are determined based on the two aforementioned tuning strategies, fixed points theory (FPT) and stability maximization criterion (SMC), respectively. And light will be shed onto the influence of negative stiffness on the control performance of DVAs and the allowable bounds on negative stiffness will be also predicted for both types of NSDVAs relevant to each optimization criterion. Finally, NSDVA-I and NSDVA-II will be compared with each other in different excitation scenarios for the first time.

This paper is organized as follows. In the next section, mathematical modeling of both NSDVA-I and NSDVA-II implementing on a SDOF primary system is first presented and a stability analysis is performed. In Sections 3 and 4, the optimal parameters of NSDVAs are analytically derived according to two aforementioned criteria, respectively. Finally, simulation results and numerical analyses are given in Section 5 in order to underline the effect of negative stiffness and to compare the control performance of different DVAs.

2. Mathematical modeling

2.1. NSDVA-I

A SDOF undamped primary system attached with a DVA-I is presented in Fig. 1a and Fig. 1b illustrates the coupled system with NSDVA-I, which is based on the classic DVA with a supplementary negative element locating between the secondary mass and the base. With an excitation force $F(t)$ exerted on the primary system, the dynamics of the two DOF system in Fig. 1b can be described by the equations of motion:

$$m_1\ddot{x}_1 = k_2(x_2 - x_1) + c_2(\dot{x}_2 - \dot{x}_1) - k_1x_1 + F(t) \tag{1a}$$

$$m_2\ddot{x}_2 = k_2(x_1 - x_2) + c_2(\dot{x}_1 - \dot{x}_2) - k_nx_2 \tag{1b}$$

where x_1 and x_2 are the displacements of the main and secondary mass, respectively, and the dot represents differentiation with respect to the actual time t. m_1 and k_1 are the mass and mechanical stiffness of the primary system. m_2, c_2 and k_2 stand for the mass, viscous damping coefficient and mechanical stiffness of the DVA. k_n denotes the grounded negative stiffness.

Denoted by ω_1, ω_2 and ξ, the natural frequencies of the main system and of the DVA and the mechanical

damping ratio of DVA are expressed by, respectively:

$$\omega_1 = \sqrt{\frac{k_1}{m_1}}, \quad \omega_2 = \sqrt{\frac{k_2}{m_2}}, \quad \xi = \frac{c_2}{2\sqrt{k_2 m_2}}. \tag{2}$$

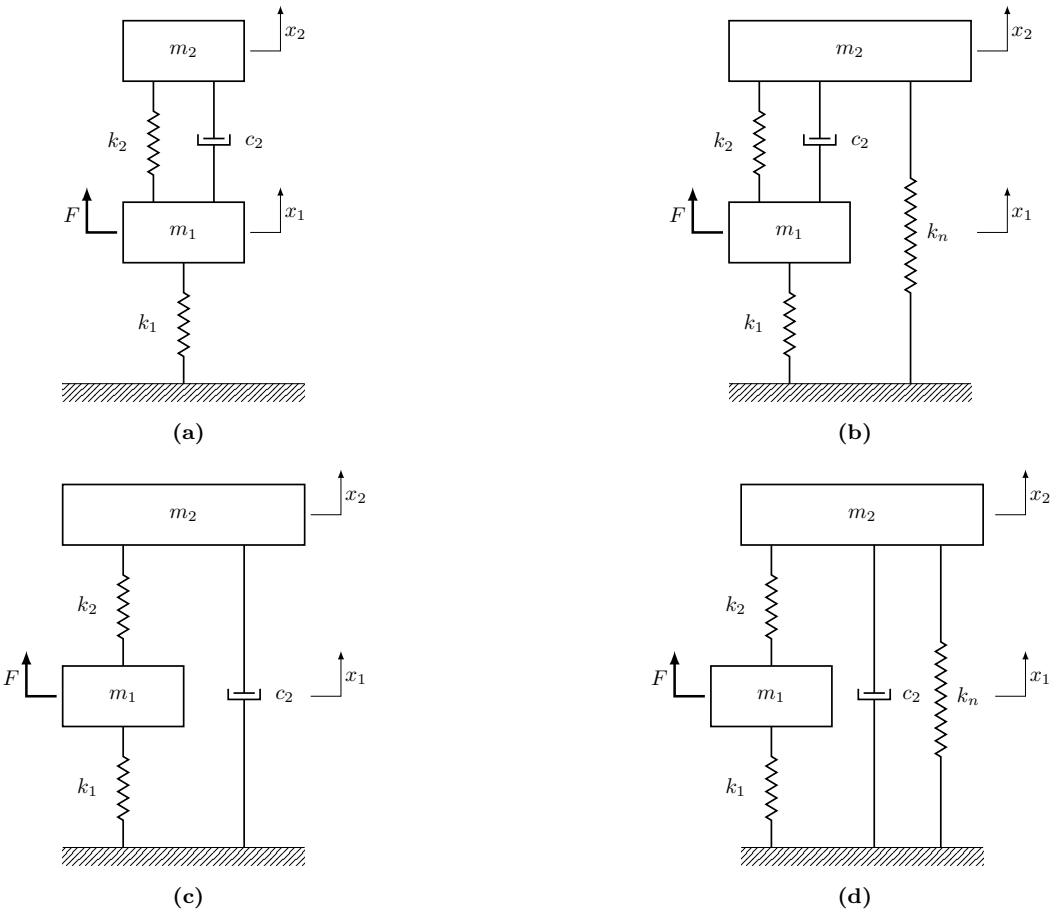

Fig. 1. Schematic diagrams of a SDOF undamped primary system controlled by four types of absorber under direct force excitation: (a) DVA-I; (b) NSDVA-I; (c) DVA-II; (d) NSDVA-II.

Then, two common tuning parameters of DVAs, the mass ratio μ and the frequency tuning ratio f between secondary and primary systems, can be defined as:

$$\mu = \frac{m_2}{m_1}, \quad f = \frac{\omega_2}{\omega_1}. \tag{3}$$

Furthermore, an additional dimensionless parameter β is herein introduced, which is defined as the ratio of negative stiffness and the mechanical stiffness of primary system:

$$\beta = \frac{k_n}{k_1} \tag{4}$$

with $\beta \leq 0$. Rescaling the time by $t = \tau/\omega_1$, one has:

$$\frac{d}{dt} = \omega_1 \frac{d}{d\tau}, \quad \frac{d^2}{dt^2} = \omega_1^2 \frac{d^2}{d\tau^2}. \tag{5}$$

By substituting Eqs. (2)-(5) into Eq. (1), the equations of motion (1) reduce to

$$x_1'' + x_1 + \mu x_2'' + \beta x_2 = F(\tau)/k_1 \tag{6a}$$

$$x_2'' + 2\xi f(x_2' - x_1') + f^2(x_2 - x_1) + \frac{\beta}{\mu} x_2 = 0 \tag{6b}$$

where the prime in the superscript indicates differentiation with respect to the rescaled time τ. The dimensionless frequency variable, complex magnitudes of displacement x_1 and external force $F(\tau)$ are denoted by $\bar{s}$, X_1 and F, respectively. The transfer function $G_I(\bar{s})$ relating the static displacement of primary system, F/k_1, and the displacement of primary system, X_1, can be obtained by transforming Eq. (6) in the Laplace domain:

$$G_I(\bar{s}) = \frac{X_1}{F/k_1} = \frac{\mu\bar{s}^2 + 2\mu\xi f\bar{s} + \beta + \mu f^2}{\mu\bar{s}^4 + 2\mu\xi f(1+\mu)\bar{s}^3 + (\beta + \mu + \mu f^2 + \mu^2 f^2)\bar{s}^2 + 2\mu\xi f(1+\beta)\bar{s} + \beta + \mu f^2(1+\beta)} \tag{7}$$

where F/k_1 corresponds to the static deformation amplitude of primary system when controlled by a classic DVA, namely $\beta = 0$. It is worth noting that as a negative stiffness is present, the static displacement of primary system is no longer equal to F/k_1, as evident from $G_I(\bar{s} = 0) \neq 1$.

2.2. NSDVA-II

Fig. 1c illustrates the undamped primary system controlled by a non-traditional DVA, and Fig. 1d represents the coupled system relevant to NSDVA-II. Similarly, the dynamics of coupled system in Fig. 1d can be formulated as:

$$m_1\ddot{x}_1 = k_2(x_2 - x_1) - k_1x_1 + F(t) \tag{8a}$$

$$m_2\ddot{x}_2 = k_2(x_1 - x_2) - k_nx_2 - c_2\dot{x}_2 \tag{8b}$$

By taking the same procedure as in subsection 2.1, Eq. (8) can be recast into a dimensionless form:

$$x_1'' + (1+\mu f^2)x_1 - \mu f^2 x_2 = F(\tau)/k_1 \tag{9a}$$

$$x_2'' + 2\xi f x_2' + f^2(x_2 - x_1) + \frac{\beta}{\mu}x_2 = 0 \tag{9b}$$

In this scenario, the transfer function $G_{II}(\bar{s})$ from the static displacement of primary system, F/k_1, to the displacement of primary system, X_1, is described by:

$$G_{II}(\bar{s}) = \frac{X_1}{F/k_1} = \frac{\mu\bar{s}^2 + 2\mu\xi f\bar{s} + \beta + \mu f^2}{\mu\bar{s}^4 + 2\mu\xi f\bar{s}^3 + (\beta + \mu + \mu f^2 + \mu^2 f^2)\bar{s}^2 + 2\mu\xi f(1+\mu f^2)\bar{s} + \beta + \mu f^2(1+\beta)} \tag{10}$$

It is apparent that the transfer function of coupled system without negative stiffness can be achieved by vanishing β in Eq. (7) or (10). Moreover, the primary system coupled with either a NSDVA-I or a NSDVA-II has the same expression of static displacement, as $G_I(\bar{s} = 0) = G_{II}(\bar{s} = 0)$.

2.3. Stability analysis

In light of the inclusion of negative stiffness, it is of a special importance to specify the allowable bound on the value of negative stiffness, within which the coupled system remains stable. Considering that stability analysis of such kind of system is rare in the current literature, therefore, one of the major contribution of this present paper is to conduct a systematic study on stability issue of primary system coupled with different types of NSDVA and in the two aforementioned excitation scenarios.

According the Routh-Hurwitz stability criterion, a system is asymptotically stable if and only if all its eigenvalues lie in the left half of the complex plane. Denoted by λ, eigenvalues can be determined by the characteristic polynomial $P(\lambda)$ of the two DOF system in the form of:

$$P(\lambda) = \lambda^4 + \delta_1\lambda^3 + \delta_2\lambda^2 + \delta_3\lambda + \delta_4 \tag{11}$$

and the stability of coupled system is guaranteed when the following necessary and sufficient conditions are satisfied:

$$\delta_1 > 0, \quad \delta_3 > 0, \quad \delta_4 > 0, \quad \delta_1\delta_2\delta_3 > \delta_3^2 + \delta_1^2\delta_4. \tag{12}$$

where all real coefficients of the characteristic polynomial $P(\lambda)$ correspond to the ones in the denominator of the transfer function, $G_I(\bar{s})$ or $G_{II}(\bar{s})$, recasting into the monic form. Therefore, these coefficients are given by

- NSDVA-I:

$$\delta_1 = 2\xi f(1+\mu), \quad \delta_2 = 1 + \frac{\beta}{\mu} + (1+\mu)f^2, \quad \delta_3 = 2\xi f(1+\beta), \quad \delta_4 = \frac{\beta}{\mu} + (1+\beta)f^2. \tag{13}$$

- NSDVA-II:

$$\delta_1 = 2\xi f, \quad \delta_2 = 1 + \frac{\beta}{\mu} + (1+\mu)f^2, \quad \delta_3 = 2\xi f(1+\mu f^2), \quad \delta_4 = \frac{\beta}{\mu} + (1+\beta)f^2. \tag{14}$$

By substituting Eq. (13) or (14) into Eq. (12), a unique constraint on the negative stiffness ratio β for both types of NSDVAs can be achieved as follows:

$$\beta > -\frac{\mu f^2}{\mu f^2 + 1} = -1 + \frac{1}{\mu f^2 + 1} \tag{15}$$

where the expression of lower bound on β is implicit due to the probable dependence between the frequency tuning ratio f and the negative stiffness ratio β. Nevertheless, it is evident from Eq. (15) that β should be always greater than -1 for any positive mass ratio μ, signifying that the absolute value of negative stiffness k_n should be always inferior to that of primary system k_1. The explicit expression for lower limit of β will be derived in the following study under the condition that the analytical formulation of frequency tuning ratio f is sought and expressed as a function of β.

3. Optimization of NSDVA-I

In this section, the primary system undergoes a sinusoidal or transient disturbance and the parameters of NSDVA-I are tuned successively by the FPT and SMC. Moreover, the permissible bound on β will be specified in each scenario and an optimal value of β will be also defined in the harmonic case.

3.1. Harmonic excitation scenario

Considering that the primary system is harmonically excited at the forcing frequency ω, its squared amplitude of FRF can be written by substituting $\bar{s} = j\omega/\omega_1 = j\alpha$ into Eq. (7):

$$G_I^2(\Omega) = \left|\frac{X_1}{F/k_1}\right|^2 = \frac{A + 4\xi^2 B}{C + 4\xi^2 D} \tag{16}$$

with $j = \sqrt{-1}$ and α designating the excitation frequency normalized by the natural frequency of primary system. And the four components are given by:

$$\begin{aligned} A &= \left[\beta + \mu(\phi - \Omega)\right]^2, & B &= \mu^2\phi\Omega, \\ C &= \left[\left[\beta + \mu(\phi - \Omega)\right](1 - \Omega) + \mu\phi(\beta - \mu\Omega)\right]^2, & D &= \mu^2\phi\Omega\left(1 - \Omega + \beta - \mu\Omega\right)^2. \end{aligned} \tag{17}$$

where two intermediate parameters are introduced for the purpose of brevity, i.e.:

$$\phi = f^2, \quad \Omega = \alpha^2. \tag{18}$$

147 *3.1.1. Optimal tuning based on fixed points theory*

148 Fig. 2 depicts several normalized frequency responses of primary system coupled with a NSDVA-I with different
149 damping ratios. One can tell that there exist two fixed points, denoted by P and Q, whose abscissas are
150 independent of the mechanical damping ratio ξ. In order to locate their abscissas, two extreme scenarios are
151 considered, $\xi = 0$ and $\xi \to \infty$, where the squared amplitudes of FRF can be simplified as:

$$G_I^2\Big|_{\xi=0} = \frac{A}{C}, \quad G_I^2\Big|_{\xi\to\infty} = \frac{B}{D}. \tag{19}$$

Equating the two previous expressions results in

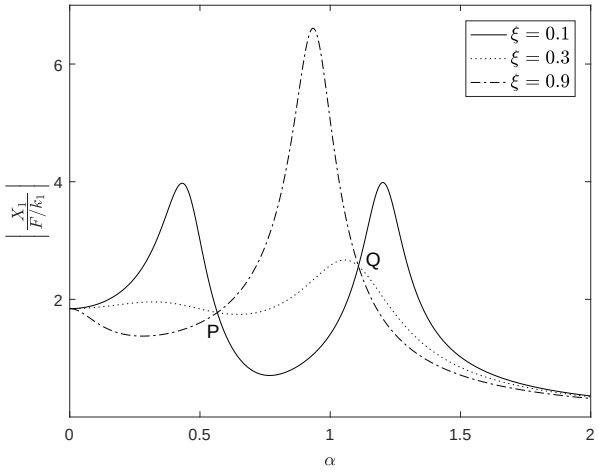

Fig. 2. Existence of fixed points in frequency response of a SDOF undamped primary system attached with a NSDVA-I. $\mu = 0.05$, $\beta = -0.1$ and $f = 1.6$. Solid line: $\xi = 0.1$, dotted line: $\xi = 0.3$, dash-dotted line: $\xi = 0.9$.

152

$$\frac{\beta + \mu(\phi - \Omega)}{\big[\beta + \mu(\phi - \Omega)\big](1 - \Omega) + \mu\phi(\beta - \mu\Omega)} = \pm\frac{1}{1 - \Omega + \beta - \mu\Omega} \tag{20}$$

153 The positive sign does not conduct to meaningful results, while the negative sign leads to a quadratic equation
154 in Ω:

$$(\mu^2 + 2\mu)\Omega^2 - 2(\beta + \mu + \beta\mu + \mu\phi + \mu^2\phi)\Omega + \beta^2 + 2\beta + 2\mu\phi(1 + \beta) = 0 \tag{21}$$

155 from which the abscissas at the two fixed points satisfy the following condition:

$$\Omega_P + \Omega_Q = \frac{2(\beta + \mu + \beta\mu + \mu\phi + \mu^2\phi)}{\mu^2 + 2\mu} \tag{22}$$

156 Furthermore, the vibration magnitudes at Ω_P and Ω_Q should be equalized, namely:

$$G_I\Big|_{\xi\to\infty,\Omega=\Omega_P} = G_I\Big|_{\xi\to\infty,\Omega=\Omega_Q} \tag{23}$$

157 yielding another constraint on abscissas at fixed points that:

$$\Omega_P + \Omega_Q = \frac{2(1 + \beta)}{1 + \mu} \tag{24}$$

158 The combination of Eqs. (22) and (24) gives the optimal frequency tuning ratio $f_{\mathrm{I,fpt}}$ as a function of the mass
159 ratio μ and the negative stiffness ratio β:

$$f_{\mathrm{I,fpt}} = \sqrt{\phi_{\mathrm{I,fpt}}} \quad = \sqrt{\frac{\mu - \beta}{\mu(1 + \mu)^2}} \tag{25}$$

The back substitution of Eq. (25) into (21) and solving the quadratic equation yield the abscissas at two fixed points, respectively,

$$\Omega_P = \frac{\mu(\mu+2)(\beta+1) - \sqrt{\mu(\mu+2)(\mu-\beta)^2}}{\mu(\mu+1)(\mu+2)}, \quad \Omega_Q = \frac{\mu(\mu+2)(\beta+1) + \sqrt{\mu(\mu+2)(\mu-\beta)^2}}{\mu(\mu+1)(\mu+2)}. \tag{26}$$

Then, the optimal maximum amplitude of FRF can be obtained as:

$$G_{\mathrm{I,fpt}} = G_I\Big|_{\xi\to\infty,\Omega=\Omega_P} = G_I\Big|_{\xi\to\infty,\Omega=\Omega_Q} = \sqrt{\frac{\mu(\mu+2)}{(\mu-\beta)^2}} \tag{27}$$

Up to now, the only unknown tuning parameter is the absorber damping ratio ξ, and a direct way of determining its optimal value is to set as zero the partial derivative of FRF (16) with respect to Ω at fixed points P and Q, which could be cumbersome in some cases. Therefore, the Brock's approach [29] is adopted in this paper to obtain the optimal damping ratio ξ in avoidance of the tedious derivatives. Denoting the optimal squared magnitude at fixed points by $\hbar = G^2_{\mathrm{I,fpt}}$, the mechanical damping ratio ξ can be expressed as a function of this amplitude in such a way that:

$$4\xi^2 = -\frac{A - \hbar C}{B - \hbar D} \tag{28}$$

Instead of imposing the horizontal tangent constraint at the fixed point P, we consider an adjacent point, $\tilde{P}$ of abscissa $\Omega = \Omega_P + \epsilon$ with ϵ being the small perturbation in Ω, and equating its magnitude to $\hbar$ at fixed points, i.e.:

$$4\xi^2 = -\frac{A - \hbar C}{B - \hbar D}\Big|_{\Omega=\Omega_P+\epsilon} = \frac{n_0 + n_1\epsilon + n_2\epsilon^2 + \dots}{d_0 + d_1\epsilon + d_2\epsilon^2 + \dots} \tag{29}$$

where the coefficients of ϵ are dependent of μ, β, ϕ and $\hbar$. It can be proven that the constant terms n_0 and d_0 are equal to zero when $\phi = \phi_{I,fpt}$, $\hbar = \hbar_{\mathrm{opt}}$ and $\Omega = \Omega_P$ or Ω_Q. Therefore, the fraction n_0/d_0 is of intermediate form 0/0 and the optimal damping ratio can be obtained by approaching $\epsilon \to 0$. According to the *de L'Hospital*'s rule, one has:

$$4\xi^2_{\mathrm{I,fpt}} = \lim_{\epsilon\to 0} 4\xi^2 = \frac{n_1}{d_1} \tag{30}$$

with the numerator and denominator given by:

$$\begin{aligned} n_1 &= n_{10} + n_{11}\Omega + n_{12}\Omega^2 + n_{13}\Omega^3 \\ d_1 &= d_{10} + d_{11}\Omega + d_{12}\Omega^2 \end{aligned} \tag{31}$$

where all coefficients are expressed as:

$$\begin{cases} n_{10} = -2\,\hbar\,\mu^2\,(\mu+1)\,(\beta+1)\,\phi^2 - 2\,\mu\left(\hbar\,\beta^2 + 2\,\hbar\,\beta\,\mu + 2\,\hbar\,\beta + \hbar\,\mu - \mu\right)\phi - 2\,\beta\,(\hbar\,\beta + \hbar\,\mu - \mu) \\ n_{11} = 2\,\hbar\,\mu^2\,(\mu+1)^2\,\phi^2 + 4\,\hbar\,\mu\left(2\,\beta\,\mu + \mu^2 + \beta + 2\,\mu\right)\phi + 2\,\hbar\,\beta^2 + 8\,\hbar\,\beta\,\mu + 2\,\hbar\,\mu^2 - 2\,\mu^2 \\ n_{12} = -6\,\hbar\,\mu\left(\mu^2\phi + \mu\,\phi + \beta + \mu\right) \\ n_{13} = 4\,\hbar\,\mu^2 \\ d_{10} = -\mu^2\phi\left(\hbar\,\beta^2 + 2\,\hbar\,\beta + \hbar - 1\right) \\ d_{11} = 4\,\hbar\,\mu^2\phi\,(\mu+1)\,(\beta+1) \\ d_{12} = -3\,\hbar\,\mu^2\phi\,(\mu+1)^2 \end{cases} \tag{32}$$

The optimal damping ratio $\xi_{\mathrm{I,fpt}}$ can be then computed by substituting the optimal frequency tuning ratio (25), frequencies at fixed points (26) and peak magnitude (27) into Eq. (30). Clearly, two quasi-optimal solutions of

$\xi_{\mathrm{I,fpt}}$ can be obtained at the two fixed points, which are denoted by ξ_P and ξ_Q and are slightly different with each other. Finally, their root mean square value is accepted as the optimal mechanical damping ratio, i.e.:

$$\xi_{\mathrm{I,fpt}} = \sqrt{\frac{\xi_P^2 + \xi_Q^2}{2}} = \sqrt{\frac{\mu(2\beta\mu + 5\beta + 3)(\mu - \beta)^3}{4(\mu+1)\Big[\mu(\mu+2)(\beta+1)^2(\mu-\beta)^2 - (\mu-\beta)^4\Big]}} \tag{33}$$

By imposing $\beta = 0$, Eq. (33) reduces to $\sqrt{3\mu/8(1+\mu)}$, which is exactly the classic expression derived in [5] for the DVA-I without negative stiffness.

3.1.2. Lower limit and optimal value of β

By substituting the optimal frequency tuning ratio (25) into the general stability condition (15), an inequality on β can be obtained:

$$\beta^2 - (\mu^2 + 3\mu)\beta - \mu < 0 \tag{34}$$

suggesting that β should locate within the interval $(\beta^-_{\mathrm{I,fpt}}, \beta^+_{\mathrm{I,fpt}})$, with the lower and upper limits defined by:

$$\beta^-_{\mathrm{I,fpt}} = \frac{\mu^2 + 3\mu - \sqrt{(\mu^2+3\mu)^2 + 4\mu}}{2}, \quad \beta^+_{\mathrm{I,fpt}} = \frac{\mu^2 + 3\mu + \sqrt{(\mu^2+3\mu)^2 + 4\mu}}{2}. \tag{35}$$

It is noticeable that $\beta^+_{\mathrm{I,fpt}} > 0$ and $\beta^-_{\mathrm{I,fpt}} > -1$ always hold for any positive μ. The allowable bound on β is then reduced to:

$$\beta \in (\beta^-_{\mathrm{I,fpt}}, 0] \tag{36}$$

Fig. 3 depicts the frequency response surface of primary system against the dimensionless excitation frequency α and the negative stiffness ratio β with absorber parameters tuned by the fixed points theory. The curve C1 corresponds to the frequency response curve of a classic DVA-I, namely $\beta = 0$. It is apparent that the inclusion of negative stiffness does contribute to the decreasing of peak vibration amplitude and the increasing of absorbing frequency range. Nevertheless, the vibration amplitude at $\alpha = 0$, i.e. static displacement $X_{I,st}$ of primary system attached with a NSDVA-I, increases monotonically as the negative stiffness ratio β approaches to its lower limit $\beta^-_{\mathrm{I,fpt}}$, which is in contrast with the trend of the magnitude at fixed points. Therefore, it could be postulated that the optimal negative stiffness ratio $\beta_{\mathrm{I,fpt}}$ is achieved when are equalized the static amplitude of primary system $X_{I,st}$ and the peak magnitude $\hbar$ given in Eq. (27). The static amplitude of primary system $X_{I,st}$ can be determined by imposing $\Omega = 0$ in Eq. (16), leading to:

$$X_{I,st} = G_I\Big|_{\Omega=0} = \frac{\mu + (\mu^2 + 2\mu)\beta}{\mu + (\mu^2+3\mu)\beta - \beta^2} \tag{37}$$

It is worth noting that $X_{I,st}$ deviates from unity in the presence of negative stiffness (namely $\beta \neq 0$), which designates that the static displacement of primary system is no longer controlled solely by the mechanical property of primary system but also influenced by the secondary oscillator. Equating Eqs. (27) and (37) yields four rational values of $\beta_{\mathrm{I,fpt}}$, respectively:

$$\begin{aligned} \beta_1 &= \frac{\mu^2 + 3\mu - (\mu+1)\sqrt{\mu^2+2\mu}}{2 - (\mu+1)^2}, \quad \beta_2 = \frac{\mu^2 + 3\mu + (\mu+1)\sqrt{\mu^2+2\mu}}{2 - (\mu+1)^2}, \\ \beta_3 &= \frac{\mu^2 + 2\mu - (\mu+1)\sqrt{\mu^2+2\mu}}{\mu+2}, \quad \beta_4 = \frac{\mu^2 + 2\mu + (\mu+1)\sqrt{\mu^2+2\mu}}{\mu+2}. \end{aligned} \tag{38}$$

where β_2 and β_4 are always positive for a mass ratio $\mu < 0.25$ which covers the most engineering applications in practice. Furthermore, β_1 is always inferior to the lower bound $\beta^-_{\mathrm{I,fpt}}$ for any positive μ, with which the coupled system becomes unstable. Finally, β_3 satisfies the following condition:

$$-1 < \beta^-_{\mathrm{I,fpt}} < \beta_3 < 0 \tag{39}$$

which clearly suggests the existence of an optimal negative stiffness ratio $\beta_{\mathrm{I,fpt}}$ within the stable region, which is formulated as:

$$\beta_{\mathrm{I,fpt}} = \beta_3 \quad = \frac{\mu^2 + 2\mu - (\mu+1)\sqrt{\mu^2+2\mu}}{\mu+2} \tag{40}$$

Marked by C2, the frequency response of primary system with the optimal value $\beta_{\mathrm{I,fpt}}$ is drawn in Fig. 3, where an equilibrium is established between the increasing of static displacement and the decreasing of vibration amplitude at fixed points as the negative stiffness goes up to its lower limit.

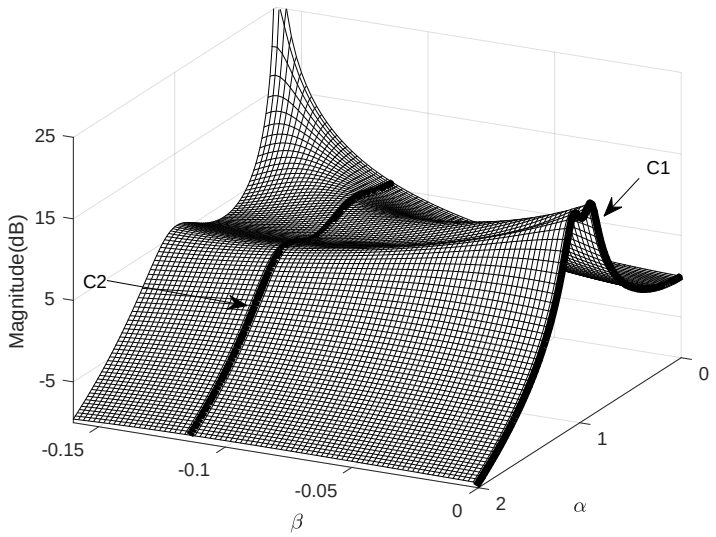

Fig. 3. Frequency response of primary system attached with a NSDVA-I versus the dimensionless frequency α and the negative stiffness ratio β with $\mu = 0.05$. Curve C1: $\beta = 0$, C2: $\beta = \beta_{\mathrm{I,fpt}}$.

Fig. 4 depicts the evolution of peak vibration amplitude of primary system controlled by a NSDVA-I (marked by black solid curve) with respect to the stiffness ratio β when optimized by the fixed points theory. A minimum is observed in the peak amplitude curve within the stability region, at which the optimal negative stiffness ratio is defined and coincides with the one predicted by Eq. (40).

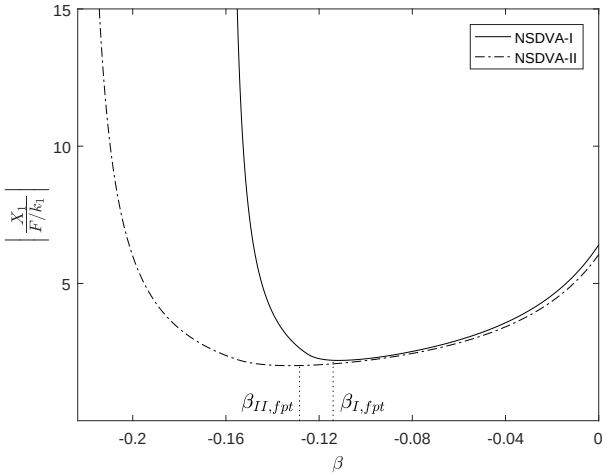

Fig. 4. Evolution of normalized peak vibration amplitude of primary system with respect to negative stiffness ratio β in the optimal scenario relevant to fixed points theory with given mass ratio $\mu = 0.05$. Solid line: NSDVA-I, dash-dotted line: NSDVA-II.

3.2. Transient excitation scenario

In practice, there exists other performance assessment than optimizing the steady state frequency response of primary system, e.g. shaping its transient response optimally in terms of fast attenuation and low peak response. As presented in the Introduction, this design objective could be achieved by tuning the NSDVA according to the stability maximization criterion.

3.2.1. Optimal tuning based on stability maximization criterion

Give that the coupled system is of two DOFs, there exist four eigenvalues for its characteristic polynomial, denoted by λ_1, λ_2, λ_3 and λ_4. Therefore, the transient response of primary system under free vibration can be expressed in the form of:

$$x_1(\tau) = A_1 e^{\lambda_1 \tau} + A_2 e^{\lambda_2 \tau} + A_3 e^{\lambda_3 \tau} + A_4 e^{\lambda_4 \tau} \tag{41}$$

where A_1, A_2, A_3 and A_4 are coefficients in terms of rescaled time τ and are dependent of the initial state of the system. As proposed in [30], a performance index is defined as the absolute value of the maximal real part of all eigenvalues, i.e.:

$$\Lambda = -\max_i \left\{ \mathrm{Re}(\lambda_i) \right\} \tag{42}$$

which indicates the slowest speed of convergence of the free vibration response and is termed as the degree of stability. Therefore, the stability maximization criterion aims at maximizing the degree of stability Λ, namely all eigenvalues should locate as far as possible away from the imaginary axis in the left half complex plane.

As stated in [30], the design objective is fulfilled when the eigenvalues of coupled system take the form of a double pair of complex conjugates. Denoting the eigenvalues by $\lambda_1 = \lambda_3 = -p + jq$ and $\lambda_2 = \lambda_4 = -p - jq$, p must be positive in order to locate at the left half complex plane and is exactly the degree of stability Λ. Thus, the characteristic polynomial can be factorized in terms of its eigenvalues:

$$(\lambda - \lambda_1) \cdot (\lambda - \lambda_2) \cdot (\lambda - \lambda_3) \cdot (\lambda - \lambda_4) = 0 \tag{43}$$

which can be expanded and further rearranged in the polynomial form of λ as:

$$\lambda^4 + 4p\lambda^3 + (4p^2 + 2r^2)\lambda^2 + 4pr^2\lambda + r^4 = 0 \tag{44}$$

with $r = \sqrt{p^2 + q^2}$ designating the modulus of complex poles. By comparing coefficients in Eqs. (13) and (44), four conditions should be satisfied simultaneously:

$$4p = 2\xi f(1 + \mu) \tag{45a}$$

$$4p^2 + 2r^2 = 1 + \frac{\beta}{\mu} + (1 + \mu) f^2 \tag{45b}$$

$$4pr^2 = 2\xi f(1 + \beta) \tag{45c}$$

$$r^4 = \frac{\beta}{\mu} + (1 + \beta) f^2 \tag{45d}$$

which culminate into the SMC-based optimal parameters of NSDVA-II as follows:

$$f_{\mathrm{I,smc}} = \sqrt{\frac{(\mu - \beta)(1 - \beta\mu)}{\mu(1 + \beta)(1 + \mu)^2}}, \quad \xi_{\mathrm{I,smc}} = \sqrt{\frac{\mu - \beta}{(1 + \mu)(1 - \beta\mu)}}. \tag{46}$$

which distinguish from the ones obtained in the harmonic scenario. Besides, the modulus and real part of eigenvalues (i.e. degree of stability) are written as:

$$r_{\mathrm{I}} = \sqrt{\frac{1 + \beta}{1 + \mu}}, \quad \Lambda_{\mathrm{I}} = p_{\mathrm{I}} \quad = \sqrt{\frac{(\mu - \beta)^2}{4\mu(1 + \mu)(1 + \beta)}}. \tag{47}$$

240 *3.2.2. Lower bound on β*

241 With the knowledge of frequency tuning ratio $f_{\mathrm{I,smc}}$, the general stability condition (15) is always satisfied for
242 any $\beta > -1$. However, another constraint should be considered for the SMC-based optimization procedure, i.e.

$$p \leq r \tag{48}$$

243 as required by the complex pole assumption, which yields an inequality condition on β:

$$(1-4\mu)\beta^2 - 10\mu\beta + \mu^2 - 4\mu \leq 0 \tag{49}$$

244 Given that μ is usually lower than 0.25 in practical applications, a lower limit can be determined for β as:

$$-1 < \beta_{\mathrm{I,smc}}^{-} = \frac{\mu - 2\sqrt{\mu}}{1 + 2\sqrt{\mu}} < 0 \tag{50}$$

245 while the upper threshold related to Eq. (49) is always positive for any mass ratio μ. As a whole, the permissible
246 interval of negative stiffness ratio β in this scenario is described by:

$$\beta \in \left[\beta_{\mathrm{I,smc}}^{-}, 0\right] \tag{51}$$

247 The evolution of complex eigenvalues of the coupled system as a function of β is plotted in Fig. 5. One
248 can notice that as the negative stiffness ratio approaches gradually to its lower threshold $\beta_{\mathrm{I,smc}}^{-}$, the complex
249 conjugate pair of eigenvalues move away from the imaginary axis of complex plane and migrate towards the
250 real axis, designating a faster attenuation and a smaller oscillation cycle. When β arrives at its lower bound,
251 all four poles coincide with each other and become real, whose abscissa is equal to $-1/(1+2\sqrt{\mu})$ and for which
252 the ultimate mechanical damping ratio is written as:

$$\xi_{\mathrm{I,smc}}^{-} = \sqrt{\frac{2\sqrt{\mu}}{(1+\mu)(1-\mu+2\sqrt{\mu})}} \tag{52}$$

253 which clearly suggests that under no circumstance, the mechanical damping ratio of NSDVA-I tuned by the
SMC could be greater than or equal to unity for $\mu < 0.25$.

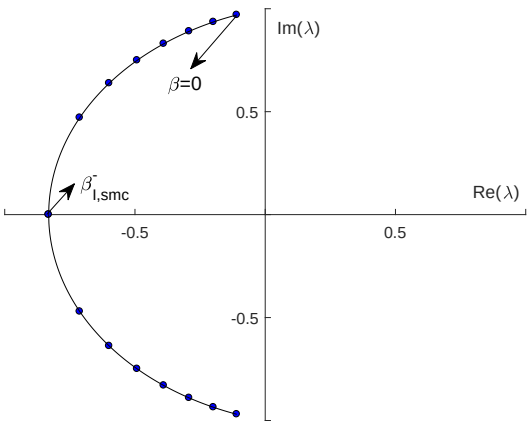

Fig. 5. Evolution of root loci of the primary system coupled with a NSDVA-I versus the negative stiffness ratio β in the SMC-based optimal scenario with given mass ratio $\mu = 0.05$. For each specific value of β, the coupled system has a double pair of complex conjugates.

254

4. Optimization of NSDVA-II

In this section, a non-traditional absorber NSDVA-II, as illustrated in Fig. 1d, is under consideration in both harmonic and free vibration cases. Although the optimization of NSDVA-II based on the fixed points theory is available in [25], its stability analysis and bound on negative stiffness ratio β had not been addressed, which will be accomplished in this paper. Furthermore, to the best knowledge of the authors, optimization based on stability maximization criterion is still lacking in the literature. Therefore, the optimization of NSDVA-II based on these two methods will be conducted by following the same procedure as in Section 3.

4.1. Harmonic excitation scenario

The primary system being excited harmonically, its squared amplitude of FRF can be cast in the form of Eq. (16) with the four coefficients expressed as:

$$\begin{aligned} A &= \left[\beta + \mu(\phi - \Omega)\right]^2, & B &= \mu^2\phi\Omega, \\ C &= \Big[\big[\beta + \mu(\phi - \Omega)\big](1 - \Omega) + \mu\phi(\beta - \mu\Omega)\Big]^2, & D &= \mu^2\phi\Omega\big(1 + \mu\phi - \Omega\big)^2. \end{aligned} \tag{53}$$

By employing the fixed points theory, the optimal frequency tuning ratio $f_{\mathrm{I,fpt}}$ is formulated as the function of the mass ratio μ and the negative stiffness ratio β:

$$f_{\mathrm{II,fpt}} = \sqrt{\frac{\mu - \beta}{\mu(1 - \mu)}} \tag{54}$$

The fixed points P and Q locate at:

$$\Omega_P = \frac{2\mu(1 - \beta) - \sqrt{2\mu(\mu - \beta)^2}}{2\mu(1 - \mu)}, \quad \Omega_Q = \frac{2\mu(1 - \beta) + \sqrt{2\mu(\mu - \beta)^2}}{2\mu(1 - \mu)}. \tag{55}$$

and the vibration amplitude at fixed points reads as:

$$G_{\mathrm{II,fpt}} = \sqrt{\frac{2\mu(1 - \mu)^2}{(\mu - \beta)^2}} \tag{56}$$

Finally, the optimal damping ratio $\xi_{\mathrm{II,fpt}}$ is determined by adopting Brock's approach, giving

$$\xi_{\mathrm{II,fpt}} = \sqrt{\frac{3\mu(1 - \beta)(\mu - \beta)^3}{4\Big[2\mu(1 - \beta)^2(\mu - \beta)^2 - (\mu - \beta)^4\Big]}} \tag{57}$$

The substitution of Eq. (54) in the general stability condition (15) leads to:

$$\beta \in (\beta^{-}_{\mathrm{II,fpt}}, 0] \tag{58}$$

with $\beta^{-}_{\mathrm{II,fpt}} = -\sqrt{\mu}$. As stated in previous section, optimal value of β can be determined by equating the static displacement of primary system and the vibration amplitude at fixed points. In this scenario, the static displacement of primary system is described by:

$$X_{II,st} = G_{II}\Big|_{\Omega=0} = \frac{\mu(1 - \beta)}{\mu - \beta^2} \tag{59}$$

Then balancing Eqs. (56) and (59) yields four possible values of $\beta_{\mathrm{II,fpt}}$, respectively:

$$\begin{aligned} \beta_1 &= \frac{-1 - (1 - \mu)\sqrt{2\mu}}{1 - 2\mu}, & \beta_2 &= \frac{-1 + (1 - \mu)\sqrt{2\mu}}{1 - 2\mu}, \\ \beta_3 &= \frac{\mu - (1 - \mu)\sqrt{2\mu}}{2 - \mu}, & \beta_4 &= \frac{\mu + (1 - \mu)\sqrt{2\mu}}{2 - \mu}. \end{aligned} \tag{60}$$

where β_2 and β_4 are greater than zero for any positive μ and $\beta_1 < \beta_{\mathrm{II,fpt}}^{-}$ always holds for $\mu < 0.25$. The last possible solution satisfies: $\beta_{\mathrm{II,fpt}}^{-} < \beta_3 < 0, \forall \mu \in (0, 0.25)$, which should be then retained. Finally, the optimal negative stiffness ratio $\beta_{\mathrm{II,fpt}}$ for the NSDVA-II is formulated as:

$$\beta_{\mathrm{II,fpt}} = \frac{\mu - (1-\mu)\sqrt{2\mu}}{2-\mu} \tag{61}$$

which is exactly the same as that proposed in [25]. Again the optimal formula (61) is validated by inspecting the frequency response of primary system with this specific value. As evident from Fig. 6, the static displacement and the vibration amplitude at fixed points are balanced in the frequency response relevant to $\beta_{\mathrm{II,fpt}}$ (denoted as C4).

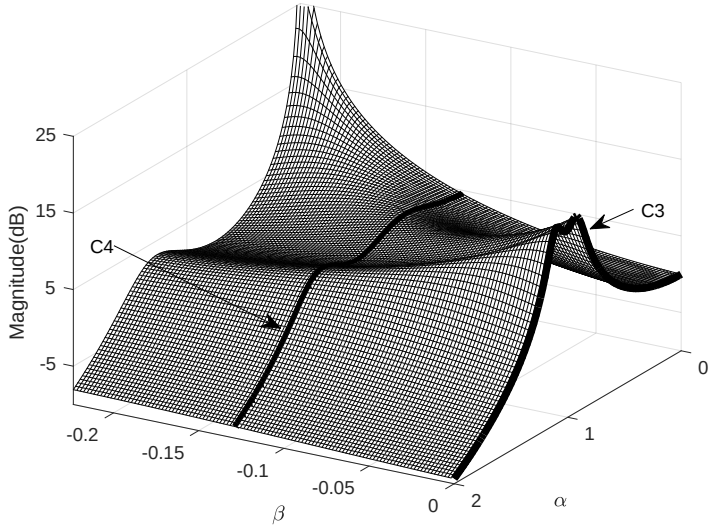

Fig. 6. Frequency response of primary system attached with a NSDVA-II versus the dimensionless frequency α and the negative stiffness ratio β with $\mu = 0.05$. Curve C3: $\beta = 0$, C4: $\beta = \beta_{\mathrm{II,fpt}}$.

4.2. Transient excitation scenario

In this scenario, the stability maximization criterion is adopted to improve the transient response of primary system connected with a NSDVA-II. By balancing the coefficients of corresponding characteristic polynomial (14) with the ones of the optimized characteristic polynomial (44), four optimality conditions should be fulfilled:

$$4p = 2\xi f \tag{62a}$$

$$4p^2 + 2r^2 = 1 + \frac{\beta}{\mu} + (1+\mu)f^2 \tag{62b}$$

$$4pr^2 = 2\xi f(1 + \mu f^2) \tag{62c}$$

$$r^4 = \frac{\beta}{\mu} + (1+\beta)f^2 \tag{62d}$$

from which one can determine the optimal tuning parameters of NSDVA-II as:

$$f_{\mathrm{II,smc}} = \sqrt{\frac{1+\beta-2\mu-\sqrt{(1+\beta)^2-4\mu}}{2\mu^2}}, \quad \xi_{\mathrm{II,smc}} = \sqrt{\frac{1-\beta-\sqrt{(1+\beta)^2-4\mu}}{2}}. \tag{63}$$

	Frequency ratio f	Mechanical damping ratio ξ	$\left\|\frac{X_1}{F/k_1}\right\|_\infty$
DVA-I [5]	$\frac{1}{1+\mu}$	$\sqrt{\frac{3\mu}{8(1+\mu)}}$	$\sqrt{\frac{\mu+2}{\mu}}$
NSDVA-I	$\sqrt{\frac{\mu-\beta}{\mu(1+\mu)^2}}$	$\sqrt{\frac{\mu(2\beta\mu+5\beta+3)(\mu-\beta)^3}{4(\mu+1)\left[\mu(\mu+2)(\beta+1)^2(\mu-\beta)^2-(\mu-\beta)^4\right]}}$	$\sqrt{\frac{\mu(\mu+2)}{(\mu-\beta)^2}}$
DVA-II [6]	$\frac{1}{\sqrt{1-\mu}}$	$\sqrt{\frac{3\mu}{4(2-\mu)}}$	$(1-\mu)\sqrt{\frac{2}{\mu}}$
NSDVA-II [25]	$\sqrt{\frac{\mu-\beta}{\mu(1-\mu)}}$	$\sqrt{\frac{3\mu(1-\beta)(\mu-\beta)^3}{4\left[2\mu(1-\beta)^2(\mu-\beta)^2-(\mu-\beta)^4\right]}}$	$(1-\mu)\sqrt{\frac{2\mu}{(\mu-\beta)^2}}$

Table 1: Optimal parameters of various types of DVAs based on the fixed points theory.

	Frequency ratio f	Damping ratio ξ	Degree of stability Λ
DVA-I [10]	$\frac{1}{1+\mu}$	$\sqrt{\frac{\mu}{1+\mu}}$	$\sqrt{\frac{\mu}{4(1+\mu)}}$
NSDVA-I	$\sqrt{\frac{(\mu-\beta)(1-\beta\mu)}{\mu(1+\beta)(1+\mu)^2}}$	$\sqrt{\frac{\mu-\beta}{(1+\mu)(1-\beta\mu)}}$	$\sqrt{\frac{(\mu-\beta)^2}{4\mu(1+\mu)(1+\beta)}}$
DVA-II [11]	$\frac{1-\sqrt{1-4\mu}}{2\mu}$	$\sqrt{\frac{1-\sqrt{1-4\mu}}{2}}$	$\sqrt{\frac{1-3\mu-(1-\mu)\sqrt{1-4\mu}}{8\mu^2}}$
NSDVA-II	$\sqrt{\frac{1+\beta-2\mu-\sqrt{(1+\beta)^2-4\mu}}{2\mu^2}}$	$\sqrt{\frac{1-\beta-\sqrt{(1+\beta)^2-4\mu}}{2}}$	$\sqrt{\frac{1+\beta-(3-\beta)\mu-(1-\mu)\sqrt{(1+\beta)^2-4\mu}}{8\mu^2}}$

Table 2: Optimal parameters of various types of DVAs according to the stability maximization criterion.

and the modulus and real part of eigenvalues (i.e. degree of stability) given by:

$$r_{\mathrm{II}} = \sqrt{\frac{1+\beta-\sqrt{(1+\beta)^2-4\mu}}{2\mu}}, \quad \Lambda_{\mathrm{II}} = p_{\mathrm{II}} \quad = \sqrt{\frac{1+\beta-(3-\beta)\mu-(1-\mu)\sqrt{(1+\beta)^2-4\mu}}{8\mu^2}}. \tag{64}$$

The authors remark that in the case of NSDVA-II, the lower limit of β is not unique for $\mu \in [0, 0.25]$ so that one should investigate the threshold of β per segment of μ. The lower bounds on negative stiffness ratio β are given directly as follows:

$$\beta^{-}_{\mathrm{II,smc}} = \begin{cases} \dfrac{\mu+2\sqrt{\mu}(5\mu-1)}{1-4\mu}, 0 \le \mu < \dfrac{1}{9}; \\ \dfrac{7\mu-1}{1-3\mu}, \dfrac{1}{9} \le \mu \le \dfrac{1}{7}; \\ 2\sqrt{\mu}-1, \dfrac{1}{5} \le \mu \le \dfrac{1}{4}. \end{cases} \tag{65}$$

whose detailed deduction is annexed in the appendix A.

At this point, it is pertinent to summarize all analytical formulae of optimal tuning parameters for both types of NSDVAs based on different optimization criteria and compare with those available in the literature. In Table

	FPT	SMC
NSDVA-I	$\beta > \beta^{-}_{\mathrm{I,fpt}} = \dfrac{\mu^2+3\mu-\sqrt{(\mu^2+3\mu)^2+4\mu}}{2}$	$\beta \geq \beta^{-}_{\mathrm{I,smc}} = \dfrac{\mu-2\sqrt{\mu}}{1+2\sqrt{\mu}}$
NSDVA-II	$\beta > \beta^{-}_{\mathrm{II,fpt}} = -\sqrt{\mu}$	$\beta \geq \beta^{-}_{\mathrm{II,smc}}$ given in Eq. (65)

Table 3: Lower bounds on negative stiffness ratio β for two types of NSDVAs based on different optimization criteria.

1 are summarized the optimal frequency tuning ratios and mechanical damping ratios of both classic DVAs and NSDVAs optimized according to the fixed points theory and the normalized vibration amplitudes at invariant points are also listed. Clearly, the optimal expressions of NSDVA-I in the second row (or NSDVA-II in the fourth row) reduce to the classic formulae of DVA-I in the first row (or DVA-II in the third row) by imposing $\beta = 0$. Similarly, the optimal tuning parameters of different DVAs calibrated by the stability maximization criterion as well as their performance indices are outlined in Table 2. Finally, in Table 3 are arranged all lower thresholds of negative stiffness ratio β for both types of NSDVAs with respect to two tuning strategies.

5. Numerical simulations and analyses

In this section, numerical simulations will be performed in order to illustrate the effect of negative stiffness on vibration control performance in both harmonic and transient scenarios by comparing with the classic DVAs. In the following study, the results are obtained with the mass ratio being $\mu = 0.05$ except for specific cases. The responses in the frequency domain are plotted directly by using the FRFs (7) and (10), meanwhile, the temporal responses are obtained by solving the dimensionless equations of motion (6) and (9) via the fourth-order Runge-Kutta method with a fixed and sufficiently small time step.

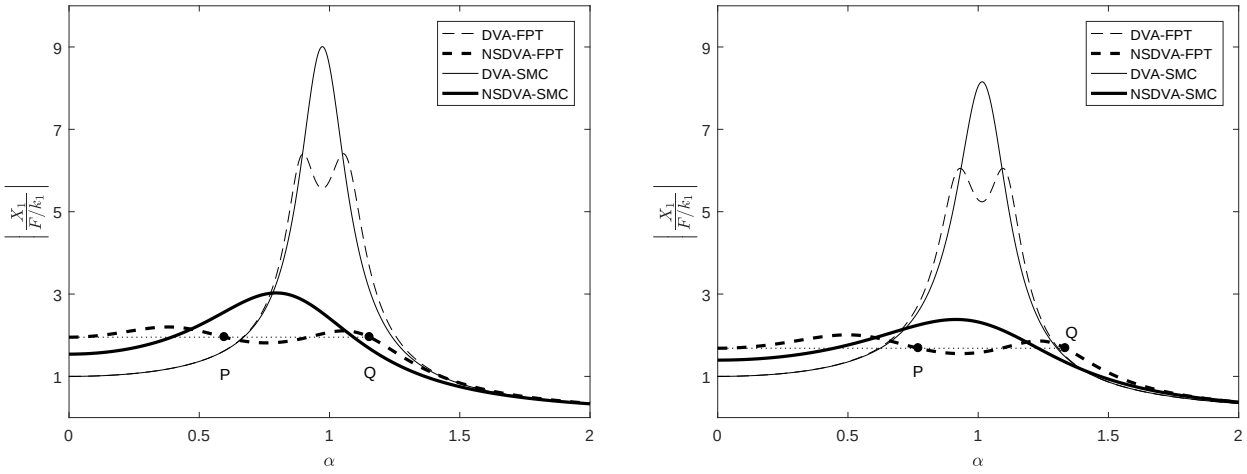

(a) DVA-I **(b)** DVA-II

Fig. 7. Frequency responses of primary structure attached to: (a) DVA-I; (b) DVA-II. Thin lines correspond to classic DVAs (namely $\beta = 0$), Thick lines are related to NSDVAs with optimal negative stiffness ratio ($\beta = \beta_{\mathrm{I,fpt}}$ or $\beta_{\mathrm{II,fpt}}$). Dashed and solid lines are responses optimized by fixed points theory and stability maximization criterion, respectively. For both configurations, vibration responses at fixed points P and Q have the same amplitude as the corresponding static displacement.

5.1. Harmonic vibration case

Fig. 7 depicts the normalized frequency responses of primary system attached with four aforementioned types of DVAs under sinusoidal force excitation. The frequency responses with DVA-I are plotted in Fig. 7a, while the performance of non-traditional DVAs is illustrated in Fig. 7b. The thin lines correspond to the absence of negative stiffness (i.e. $\beta = 0$), while the thick lines are related to the case with optimal negative stiffness ratio $\beta_{\mathrm{I,fpt}}$ or $\beta_{\mathrm{II,fpt}}$. Finally, the dashed and solid curves are relevant to DVAs optimized by FPT and SMC, respectively. It is evident that compared to the SMC, the FPT contributes to the minimizing of peak vibration amplitude of primary system in the steady state and to a relatively large frequency bandwidth of vibration suppression. Moreover, in the frequency responses related to NSDVAs with optimal negative stiffness ratio, the vibration amplitude at fixed points P and Q is equal to the static deformation (i.e. at $\alpha = 0$), validating the aforementioned postulation on optimality condition. By inspecting frequency responses relevant to DVAs and NSDVAs, one can infer that the addition of negative stiffness leads to the decrease of peak vibration amplitude, the broadening of suppression bandwidth and the left shifting of resonance area for both optimal NSDVAs. Furthermore, it is hinted that given the same mass ratio, the DVA-II (or NSDVA-II) can provide a better control performance than the DVA-I (or NSDVA-I, respectively) in terms of reducing the peak vibration amplitude of primary system.

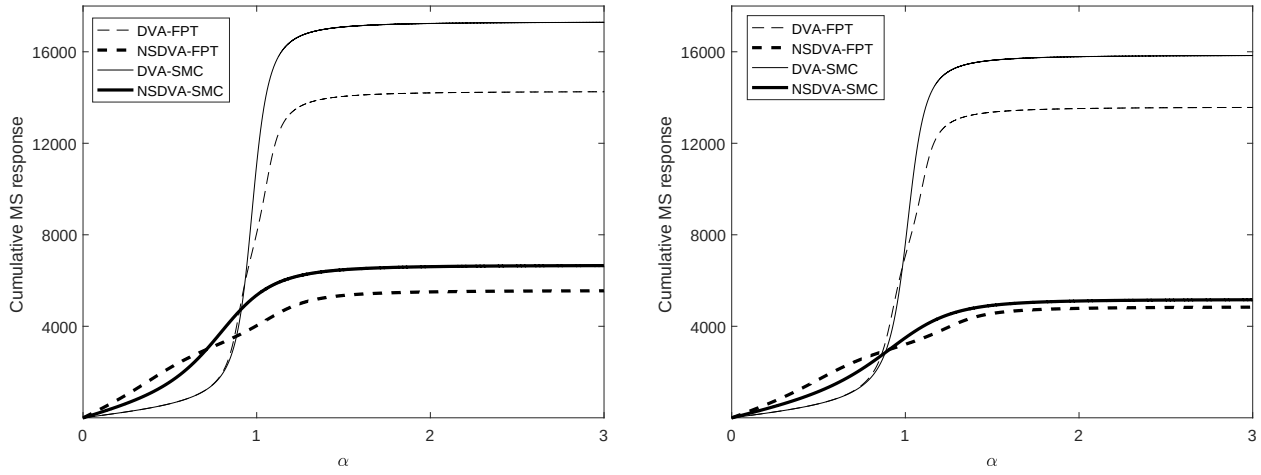

(a) DVA-I **(b)** DVA-II

Fig. 8. Cumulative mean square value of normalized displacement of primary system: (a) DVA-I; (b) DVA-II. Thin lines correspond to classic DVAs (namely $\beta = 0$), thick lines are related to NSDVAs with optimal negative stiffness ratio ($\beta = \beta_{\mathrm{I,fpt}}$ or $\beta_{\mathrm{II,fpt}}$). Dashed and solid lines are responses optimized by fixed points theory and stability maximization criterion, respectively.

The main drawback of negative stiffness is to amplify the vibration amplitude of primary system in low frequency region. Nevertheless, the justification of its use in control scheme could be twofold: improved frequency responses over a larger area around resonance as previously discussed and reduced cumulative mean square response (CMSR) of primary mass, which is illustrated in Fig. 8. The dimensionless CMSR is defined as the integrated value of squared normalized displacement of primary system over a certain frequency range [31], standing for the total kinetic energy of primary mass when undergoing a broadband excitation. Fig. 8 clearly suggests that both NSDVAs can reduce the peak value of CMSR by a factor close to 3, signifying that the use of negative stiffness can enhance significantly the system damping capability against external disturbance.

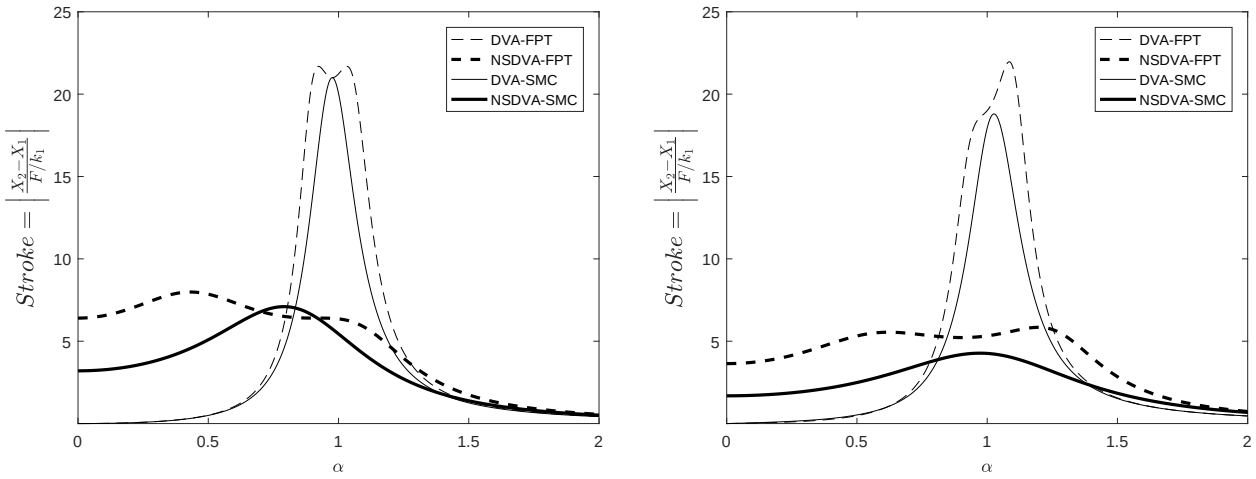

(a) DVA-I **(b)** DVA-II

Fig. 9. Frequency responses of relative displacement between primary and secondary masses: (a) DVA-I; (b) DVA-II. Thin lines correspond to classic DVAs (namely $\beta = 0$), thick lines are related to NSDVAs with optimal negative stiffness ratio ($\beta = \beta_{\mathrm{I,fpt}}$ or $\beta_{\mathrm{II,fpt}}$). Dashed and solid lines are responses optimized by fixed points theory and stability maximization criterion, respectively.

More benefit could be introduced into the control performance by using the negative stiffness. Fig. 9 demonstrates frequency responses of relative motion between primary and secondary masses, also termed as the stroke length, under harmonic force excitation. One can remark that both NSDVAs can reduce significantly the peak vibration amplitude of stroke length compared to their DVA counterparts, which facilitates their practical implementation in a more strict environment.

Nevertheless, the FPT is not oriented towards the optimization of damping ratio ξ^* of coupled system, which is defined as the minimal value of all modal damping ratios. The modal damping ratio associated with a specific eigenvalue is determined as the absolute value of ratio between its real part and its complex modulus. Therefore, increasing ξ^* leads to the decrease of damped natural frequency so that the required oscillation cycle for decaying the disturbance to zero is reduced. Fig. 10 demonstrates the evolution of system damping ratio ξ^* as a function of negative stiffness ratio β for the NSDVA-I (in Fig. 10a) and the NSDVA-II (in Fig. 10b). For both NSDVAs, FPT always yields a smaller value of ξ^* than SMC over the whole range of β, implying that SMC is more preferable for tuning NSDVAs in the case where a larger damping ratio is needed. Moreover, one can observe that the system damping value at the optimal negative stiffness ratio, $\beta_{\mathrm{I,fpt}}$ or $\beta_{\mathrm{II,fpt}}$, is not the largest, validating the fact that FPT aims at improving the steady state response instead of maximizing the damping capability.

5.2. Transient vibration case

The capability of decaying transient disturbances can be also quantified by taking the degree of stability Λ as the performance index. In fact, Λ represents the slowest exponential decay speed of transient response, therefore, a larger value of Λ corresponds to a faster decay of disturbance. Fig. 11 depicts the eigenvalues of primary system controlled by a DVA-I (in Fig. 11a) or a DVA-II (in Fig. 11b). With the definition of degree of stability given in Eq. (42), the performance indices for different DVAs read as: $\Lambda_{\mathrm{I,fpt}} = 0.061$, $\Lambda_{\mathrm{I,smc}} = 0.11$ and $\Lambda^{-}_{\mathrm{I,smc}} = 0.83$ for DVA-I based on different optimization criteria, and $\Lambda_{\mathrm{II,fpt}} = 0.067$, $\Lambda_{\mathrm{II,smc}} = 0.12$ and $\Lambda^{-}_{\mathrm{II,smc}} = 1.35$ for DVA-II with different tuning parameters. Performance indices without any superscript are

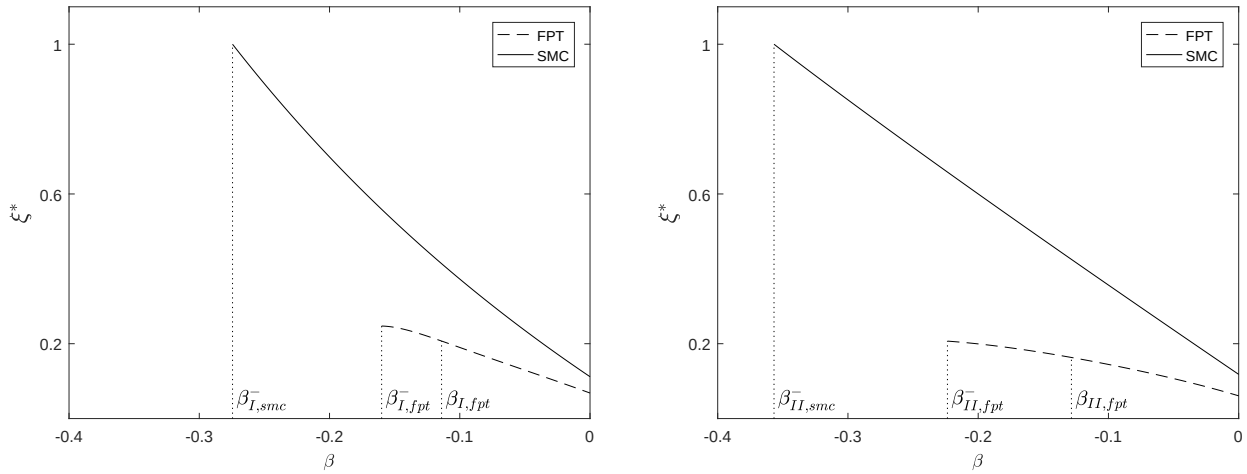

(a) NSDVA-I **(b)** NSDVA-II

Fig. 10. The fluctuation of system damping ratio ξ^* as a function of the negative stiffness ratio β: (a) NSDVA-I, (b) NSDVA-II. Dashed and solid curves are related to FPT- and SMC-based optimization, respectively.

related to DVAs without negative stiffness, while those with the superscript, −, are related to NSDVAs with critical negative stiffness ratio $\beta^-_{\mathrm{I,smc}}$ or $\beta^-_{\mathrm{II,smc}}$. It clearly suggests that the SMC always conducts to a double pair of complex eigenvalues and a larger performance index than the FPT, namely a faster convergence of transient response. In the ultimate scenario with SMC-based optimization, all the eigenvalues are coincident with each other and locates at the real axis of the complex plane, at which the largest degree of stability can be achieved. Furthermore, DVA-II has a slightly better performance index than DVA-I with $\beta = 0$, while the inclusion of negative stiffness renders the advantage claimed for DVA-II over DVA-I more significant. Precisely, an increase of 62.7% in terms of performance index is observed for the NSDVA-II when compared to NSDVA-I at their respective lower bound on β.

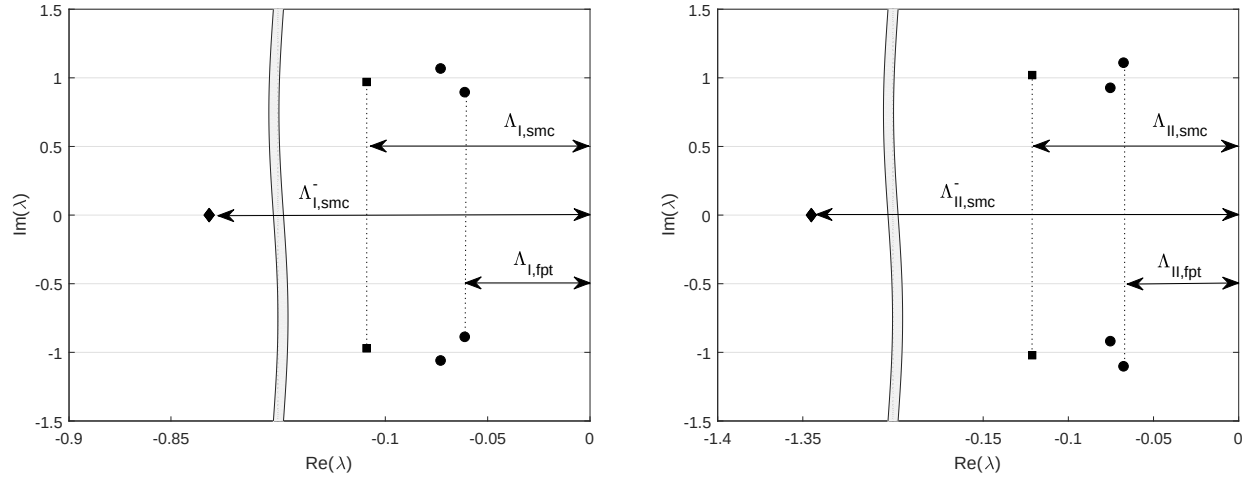

(a) DVA-I **(b)** DVA-II

Fig. 11. Root loci of primary system coupled with a: (a) DVA-I; (b) DVA-II. Circle and square markers: classic DVA optimized by FPT and SMC, respectively (i.e. $\beta = 0$); diamond marker: SMC-based NSDVA with critical negative stiffness ratio $\beta^-_{\mathrm{I,smc}}$ or $\beta^-_{\mathrm{II,smc}}$. The performance indices read as: (a) $\Lambda_{\mathrm{I,fpt}} = 0.061$, $\Lambda_{\mathrm{I,smc}} = 0.11$ and $\Lambda^-_{\mathrm{I,smc}} = 0.83$; (b) $\Lambda_{\mathrm{II,fpt}} = 0.067$, $\Lambda_{\mathrm{II,smc}} = 0.12$ and $\Lambda^-_{\mathrm{II,smc}} = 1.35$.

A numerical simulation in the temporal domain is also carried out to investigate the control performance of various DVAs with respect to transient vibration. Fig. 12 plots the temporal responses of primary system and stroke length of absorber for different configurations. The simulation is performed under free vibration (namely $F(\tau) = 0$) with a relatively large mass ratio $\mu = 0.1$ for a better visual effect. The initial states of two DOFs are imposed as: $x_1(0) = z_0 = 0.1$ and $x_1'(0) = x_2(0) = x_2'(0) = 0$. The temporal solutions related to the dimensionless ordinary differential equations (6) and (9) are obtained by adopting the fourth order Runge-Kutta method with a fixed time step 1e−4 for a simulation duration of 60. As evident from Figs. 12a and 12b, SMC and FPT render a similar attenuation performance of transient response of primary system in terms of the peak vibration amplitude and the settling time when $\beta = 0$, which is consistent with the prediction according to the performance index. Besides, the SMC-based NSDVA-II with critical negative stiffness ratio outperforms the NSDVA-I in terms of much more shorter settling time and lower peak amplitude of primary system. Finally, Figs. 12c and 12d suggest that SMC is more preferable than FPT in terms of confining the peak vibration amplitude of stroke length of DVA.

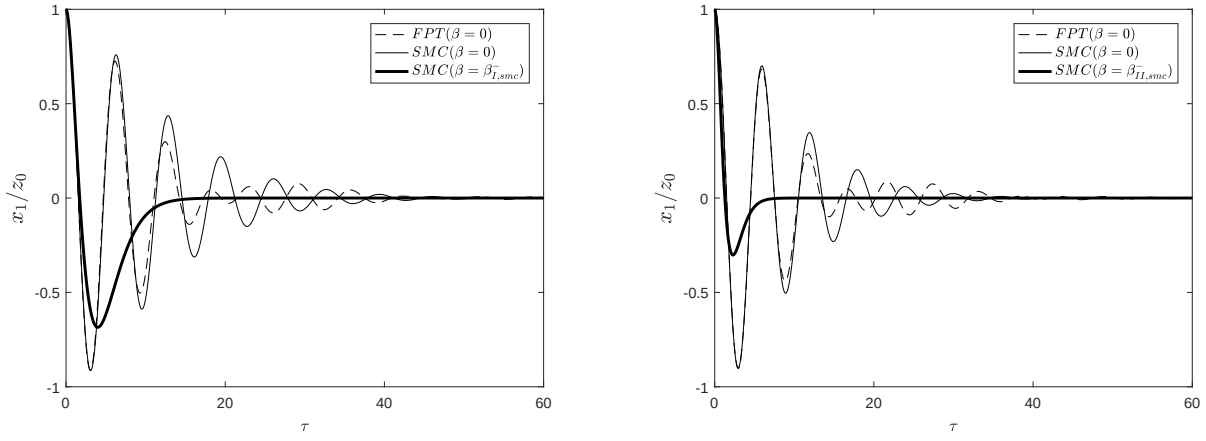

(a) DVA-I

(b) DVA-II

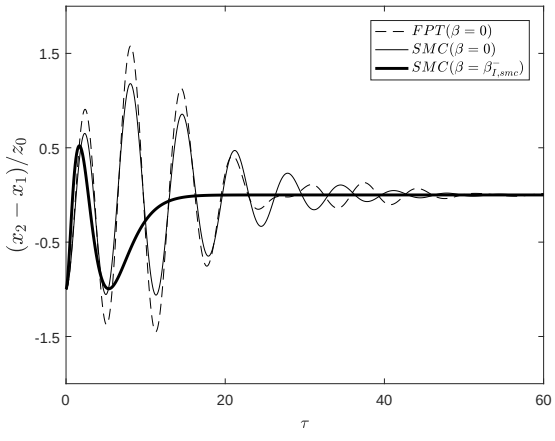

(c) DVA-I

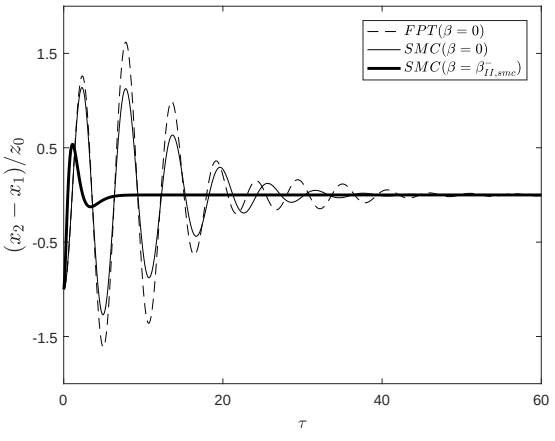

(d) DVA-II

Fig. 12. Transient responses under free vibration normalized by the initial displacement of primary system z_0: (a)-(b) displacement of primary system; (c)-(d) stroke lengths of DVAs. The mass ratio is imposed as $\mu = 0.10$. Dashed line: FPT-based DVAs (with $\beta = 0$); thin solid line: SMC-based DVAs (with $\beta = 0$); thick solid line: SMC-based NSDVAs with critical negative stiffness ratio (i.e. $\beta^-_{\mathrm{I,smc}}$ or $\beta^-_{\mathrm{II,smc}}$).

6. Conclusions

In this paper, optimization of both NSDVA-I and NSDVA-II is carried out based on two tuning strategies, fixed points theory and stability maximization criterion. Optimal parameters of frequency tuning ratio and mechanical damping ratio of absorber are derived analytically. And allowable bound on negative stiffness is specified for each NSDVA and for each optimization scenario based on the stability requirement. Besides, an optimal negative stiffness ratio is defined when the NSDVA is optimized according to the fixed points theory.

Numerical simulation results demonstrate that under harmonic excitation, the inclusion of negative stiffness can reduce significantly the maximum vibration amplitude of primary system and the stroke length of DVA and increase the frequency bandwidth of vibration suppression. Moreover, it is shown that the system damping increases as the negative stiffness approaches to its lower limit. Finally, temporal responses under free vibration suggest that in the ultimate scenario, the SMC-based NSDVAs can attenuate the transient response in an extremely short duration.

Comparisons between the two types of DVAs are also made. It is apparent that DVA-II (or NSDVA-II) can provide a better control performance than DVA-I (or NSDVA-I) in terms of confining the peak vibration amplitude of primary system and stroke length of absorber. These two types of DVAs with $\beta = 0$ have a similar performance of attenuating transient disturbance. When a negative stiffness is present, the SMC-based NSDVA-II can provide a better damping performance and have a larger permissible interval for the negative stiffness, comparing to the NSDVA-I. Therefore, the NSDVA-II can yield a more rapid convergence of transient response of both primary system and stroke length of absorber and can reduce their peak response more significantly.

7. Acknowledgements

This research did not receive any specific grant from funding agencies in the public, commercial, or not-for-profit sectors.

Appendix A Allowable interval of β for SMC-based optimization of NSDVA-II

Multiple constraints exist on the negative stiffness ratio β, as discussed one by one in the following study.

1. The stability requirement. The substitution of optimal frequency tuning ratio $f_{\mathrm{II,smc}}$ into the general stability condition (15) yields:

$$(1+\beta)^2 - 2\mu > (1+\beta)\sqrt{(1+\beta)^2 - 4\mu} \tag{A.1}$$

   which results in a possible bound on β: $\beta > \beta_1 = \sqrt{2\mu} - 1$.

2. $f_{\mathrm{II,smc}}^2 \geq 0$. This condition imposes that:

$$\left.\begin{array}{r} 1+\beta \geq 2\mu \\ (1+\beta)^2 \geq 4\mu \\ (1+\beta-2\mu)^2 \geq (1+\beta)^2 - 4\mu \end{array}\right\} \Longrightarrow \left\{\begin{array}{l} \beta \geq \beta_2 = 2\mu - 1 \\ \beta \geq \beta_3 = 2\sqrt{\mu} - 1 \end{array}\right. \tag{A.2}$$

One can tell that $\beta_3 > \beta_1 > \beta_2$ always holds for any positive $\mu \leq 0.5$ and the mass ratio should be inferior to 0.25. Up to now, the negative stiffness ratio β should be bounded by: $\beta \geq \beta_3 = 2\sqrt{\mu} - 1$.

3. The complex eigenvalue assumption $p_{\mathrm{II}}^2 \leq r_{\mathrm{II}}^2$. The inequality conducts to $t_1 \leq t_2$ with the two polynomials given by:

$$t_1 = 1 - 7\mu + \beta(1 - 3\mu), \quad t_2 = (1 - 5\mu)\sqrt{(1+\beta)^2 - 4\mu}. \tag{A.3}$$

It is remarkable that the signs of t_1 and t_2 depend on the mass ratio μ so that the lower bound on β should be deducted per segment of μ. The coefficient t_1 will be positive if $\beta > \beta_4 = (7\mu - 1)/(1 - 3\mu)$ and t_2 remains positive when μ is less than 1/5. Besides, one can tell that $\beta_3 \geq \beta_4$ for any $\mu \in [0, 1/9]$. Therefore, three possible cases where a negative stiffness could be employed in the DVA, i.e. $\beta < 0$, are listed as follows:

- Case 1: $\beta \geq \beta_3$, $\beta_3 \leq 0$, $0 \leq t_1 \leq t_2$, $\forall \mu \in \left[0, \frac{1}{9}\right]$,
- Case 2: $\beta \geq \beta_4$, $\beta_4 \leq 0$, $0 \leq t_1 \leq t_2$, $\forall \mu \in \left[\frac{1}{9}, \frac{1}{5}\right]$,
- Case 3: $\beta \geq \beta_3$, $\beta_3 \leq 0$, $t_1 \leq t_2 \leq 0$, $\forall \mu \in \left[\frac{1}{5}, \frac{1}{4}\right]$.

each of which will be investigated in order to obtain the lower bound on β with respect to the segment of mass ratio μ.

- Case 1. $\beta < 0$ always holds for $\mu \in [0, 1/9]$. Moreover, the condition $0 \leq t_1 \leq t_2$ results in:

$$(1 - 4\mu)\beta^2 - 2\mu\beta + 25\mu^2 - 4\mu \leq 0 \tag{A.4}$$

It is noticeable that the upper limit of this inequality is always positive, therefore, the corresponding bound on β is: $\beta_5 \leq \beta \leq 0$ with

$$\beta_5 = \frac{\mu + 2\sqrt{\mu}(5\mu - 1)}{1 - 4\mu} \tag{A.5}$$

With β_5 being superior to β_3 in the very range of mass ratio, the allowable bound on β is:

$$\beta_5 \leq \beta \leq 0, \forall \mu \in \left[0, \frac{1}{9}\right]. \tag{A.6}$$

- Case 2. In this range of mass ratio, the condition $0 \leq t_1 \leq t_2$ will be satisfied if $\beta \geq \beta_4$ holds. Nevertheless, β_4 will be positive when the mass ratio is greater than 1/7. Therefore, no negative stiffness could be employed in the range of $[1/7, 1/5]$ and the permissible bound on β is expressed as:

$$\beta_4 \leq \beta \leq 0, \forall \mu \in \left[\frac{1}{9}, \frac{1}{7}\right]. \tag{A.7}$$

- Case 3. The constraint of $t_1 \leq t_2 \leq 0$ gives rise to

$$\beta \leq \beta^- = \frac{\mu - 2\sqrt{\mu}(5\mu - 1)}{1 - 4\mu}, \quad \beta \geq \beta^+ = \frac{\mu + 2\sqrt{\mu}(5\mu - 1)}{1 - 4\mu} \tag{A.8}$$

In the mass ratio range of $[1/5, 1/4]$, $\beta^+ > \beta^- > 0$ always holds. Therefore, the corresponding interval of β is given as:

$$\beta_3 \leq \beta \leq 0, \forall \mu \in \left[\frac{1}{5}, \frac{1}{4}\right]. \tag{A.9}$$

Finally, the lower thresholds of negative stiffness ratio β are found for each segment of mass ratio μ and are summarized in Eq. (65).

References

[1] C. C. Chang, Mass dampers and their optimal designs for building vibration control, Engineering Structures 21 (5) (1999) 454–463. doi:10.1016/S0141-0296(97)00213-7.

[2] Q. Li, J. Fan, J. Nie, Q. Li, Y. Chen, Crowd-induced random vibration of footbridge and vibration control using multiple tuned mass dampers, Journal of Sound and Vibration 329 (19) (2010) 4068–4092. doi:10.1016/j.jsv.2010.04.013.

[3] M. H. Miguelez, L. Rubio, J. A. Loya, J. Fernandez-Saez, Improvement of chatter stability in boring operations with passive vibration absorbers, International Journal of Mechanical Sciences 52 (10) (2010) 1376–1384. doi:10.1016/j.ijmecsci.2010.07.003.

[4] S. Chesne, G. Inquiete, P. Cranga, F. Legrand, B. Petitjean, Innovative hybrid mass damper for dual-loop controller, Mechanical Systems and Signal Processing 115 (2019) 514–523. doi:10.1016/j.ymssp.2018.06.023.

[5] J. Den Hartog, Mechanical vibrations, 4th Edition, McGraw-Hill, New York, 1956.

[6] M. Z. Ren, A variant design of the dynamic vibration absorber [3], Journal of Sound and Vibration 245 (4) (2001) 762–770. doi:10.1006/jsvi.2001.3564.

[7] O. Nishihara, T. Asami, Closed-form solutions to the exact optimizations of dynamic vibration absorbers (minimizations of the maximum amplitude magnification factors), Journal of Vibration and Acoustics, Transactions of the ASME 124 (4) (2002) 576–582. doi:10.1115/1.1500335.

[8] N. D. Anh, N. X. Nguyen, Design of tmd for damped linear structures using the dual criterion of equivalent linearization method, International Journal of Mechanical Sciences 77 (2013) 164–170. doi:10.1016/j.ijmecsci.2013.09.014.

[9] N. D. Anh, N. X. Nguyen, N. H. Quan, Global-local approach to the design of dynamic vibration absorber for damped structures, JVC/Journal of Vibration and Control 22 (14) (2016) 3182–3201. doi:10.1177/1077546314561282.

[10] H. Yamaguchi, Damping of transient vibration by a dynamic absorber, Transactions of the Japan Society of Mechanical Engineers Series C 54 (499) (1988) 561–568. doi:10.1299/kikaic.54.561.

[11] P. Xiang, A. Nishitani, Optimum design and application of non-traditional tuned mass damper toward seismic response control with experimental test verification, Earthquake Engineering and Structural Dynamics 44 (13) (2015) 2199–2220. doi:10.1002/eqe.2579.

[12] K. Williams, G. Chiu, R. Bernhard, Adaptive-passive absorbers using shape-memory alloys, Journal of Sound and Vibration 249 (5) (2003) 835–848. doi:10.1006/jsvi.2000.3496.

[13] M. A. Savi, A. S. De Paula, D. C. Lagoudas, Numerical investigation of an adaptive vibration absorber using shape memory alloys, Journal of Intelligent Material Systems and Structures 22 (1) (2011) 67–80. doi:10.1177/1045389X10392612.

[14] F. Weber, C. Boston, M. Maslanka, An adaptive tuned mass damper based on the emulation of positive and negative stiffness with an mr damper, Smart Materials and Structures 20 (1). doi:10.1088/0964-1726/20/1/015012.

[15] S. Sun, J. Yang, W. Li, H. Deng, H. Du, G. Alici, T. Yan, An innovative mre absorber with double natural frequencies for wide frequency bandwidth vibration absorption, Smart Materials and Structures 25 (5). doi:10.1088/0964-1726/25/5/055035.

[16] S. B. Kumbhar, S. P. Chavan, S. S. Gawade, Adaptive tuned vibration absorber based on magnetorheological elastomer-shape memory alloy composite, Mechanical Systems and Signal Processing 100 (2018) 208–223. doi:10.1016/j.ymssp.2017.07.027.

[17] H. Xiuchang, S. Zhiwei, H. Hongxing, Optimal parameters for dynamic vibration absorber with negative stiffness in controlling force transmission to a rigid foundation, International Journal of Mechanical Sciences 152 (2019) 88–98. doi:10.1016/j.ijmecsci.2018.12.033.

[18] T. D. Le, K. K. Ahn, Experimental investigation of a vibration isolation system using negative stiffness structure, International Journal of Mechanical Sciences 70 (2013) 99–112. doi:10.1016/j.ijmecsci.2013.02.009.

[19] X. Wang, H. Liu, Y. Chen, P. Gao, Beneficial stiffness design of a high-static-low-dynamic-stiffness vibration isolator based on static and dynamic analysis, International Journal of Mechanical Sciences 142-143 (2018) 235–244. doi:10.1016/j.ijmecsci.2018.04.053.

[20] X. Sun, S. Zhang, J. Xu, Parameter design of a multi-delayed isolator with asymmetrical nonlinearity, International Journal of Mechanical Sciences 138-139 (2018) 398–408. doi:10.1016/j.ijmecsci.2018.02.026.

[21] Y. Wang, X. Jing, H. Dai, F. . Li, Subharmonics and ultra-subharmonics of a bio-inspired nonlinear isolation system, International Journal of Mechanical Sciences 152 (2019) 167–184. doi:10.1016/j.ijmecsci.2018.12.054.

[22] X. Shi, S. Zhu, Magnetic negative stiffness dampers, Smart Materials and Structures 24 (7) (2015) 072002. doi:10.1088/0964-1726/24/7/072002.

[23] F. Zhang, S. Shao, Z. Tian, M. Xu, S. Xie, Active-passive hybrid vibration isolation with magnetic negative stiffness isolator based on maxwell normal stress, Mechanical Systems and Signal Processing 123 (2019) 244–263. doi:10.1016/j.ymssp.2019.01.022.

[24] T. Mizuno, T. Toumiya, M. Takasaki, Vibration isolation system using negative stiffness, JSME International Journal, Series C: Mechanical Systems, Machine Elements and Manufacturing 46 (3) (2003) 807–812. doi:10.1299/jsmec.46.807.

[25] Y. Shen, H. Peng, X. Li, S. Yang, Analytically optimal parameters of dynamic vibration absorber with negative stiffness, Mechanical Systems and Signal Processing 85 (2017) 193–203. doi:10.1016/j.ymssp.2016.08.018.

[26] I. A. Antoniadis, S. A. Kanarachos, K. Gryllias, I. E. Sapountzakis, Kdamping: A stiffness based vibration absorption concept, JVC/Journal of Vibration and Control 24 (3) (2018) 588–606. doi:10.1177/1077546316646514.

[27] X. Huang, Z. Su, H. Hua, Application of a dynamic vibration absorber with negative stiffness for control of a marine shafting system, Ocean Engineering 155 (2018) 131–143. doi:10.1016/j.oceaneng.2018.02.047.

[28] S. Krenk, J. Høgsberg, Tuned mass absorber on a flexible structure, Journal of Sound and Vibration 333 (6) (2014) 1577–1595. doi:10.1016/j.jsv.2013.11.029.

[29] K. Liu, J. Liu, The damped dynamic vibration absorbers: Revisited and new result, Journal of Sound and Vibration 284 (3-5) (2005) 1181–1189. doi:10.1016/j.jsv.2004.08.002.

[30] S. Zhou, C. Jean-Mistral, S. Chesne, Electromagnetic shunt damping with negative impedances: Optimization and analysis, Journal of Sound and Vibration 445 (2019) 188–203. doi:10.1016/j.jsv.2019.01.014.

[31] S. Chesne, C. Collette, Experimental validation of fail-safe hybrid mass damper, JVC/Journal of Vibration and Control 24 (19) (2018) 4395–4406. doi:10.1177/1077546317724949.

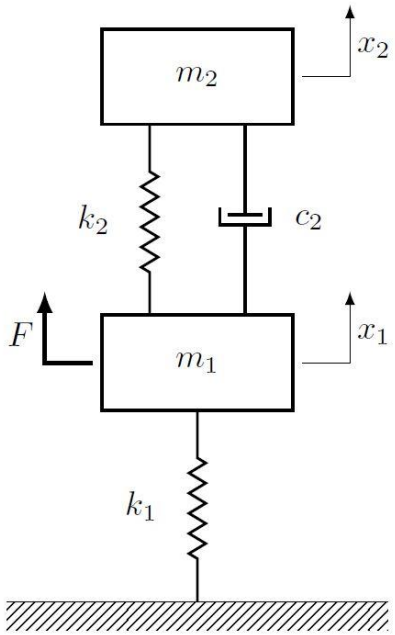

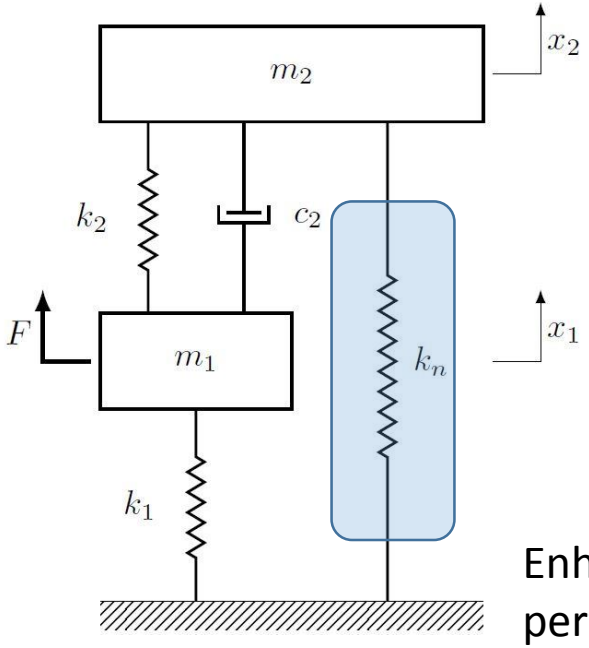

DVAs

Negative stiffness

NSDVAs

Enhanced performance of vibration control